Fig. 2. A stereoview ([001] out of the paper) of the unit-cell contents for RbNO$_3$(IV) at 298 K. A typical Rb-atom pseudocube is outlined.

about 353 K. Within this temperature (rise) interval, the relative increase of the integrated intensities for strong, low-index reflections due to the change of 'crystal perfection' would likely be considerably greater than the relative decrease of intensities due to the temperature-factor effects. This could account for the increase of intensities with temperature rise to maxima values, while beyond this region the observed decrease of intensities could be due to the temperature-factor effects alone (Fig. 1a). On subsequent cooling from 438 K, the intensities increased continuously down to room temperature, as would be expected for the temperature-factor effects alone (Fig. 1b), and would be consistent with the crystal now being closer to 'ideally imperfect'.

### References

BROWN, R. N. & MCLAREN, A. C. (1962). Acta Cryst. 15, 974–976.

BURY, P. C. & MCLAREN, A. C. (1969). Phys. Status Solidi, 31(2), 799–806.

FRANKLIN, F. Y. W. & COX, D. E. (1970). Acta Cryst. A26, 377–378.

HETTICH, A. & STEINMETZ, H. (1932). Z. Phys. 76, 688–706.

International Tables for X-ray Crystallography (1974). Vol. IV, p. 323. Birmingham: Kynoch Press.

KARPOV, S. V. & SHULTIN, A. A. (1970). Phys. Status Solidi, 39, 33–38.

KENNARD, C. H. L. (1978). Private communication, Chemistry Department, University of Queensland. (Information conveyed from S. C. KENNEDY and M. R. SNOW.)

LUCAS, B. W. (1976). J. Phys. E, 9, 262–264.

MUELLER, M. H., SIDHU, S. S., HEATON, L., HITTERMAN, R. L. & KNOTT, H. W. (1963). Report ANL-6797, p. 393. Argonne National Laboratory, Illinois.

NIMMO, J. K. (1980). Acta Cryst. A36, 830.

PAULING, L. & SHERMAN, J. (1933). Z. Kristallogr. 84, 213–216.

PLYUSCHEV, V. E., MARKINA, I. B. & SHKLOVER, L. P. (1956). Dokl. Akad. Nauk SSSR, 108, 645–647.

SCHNEIDER, C. S. (1976). Acta Cryst. A32, 375–379.

SHULL, G. G. & WOLLAN, E. O. (1956). Solid State Phys. 2, 144.

---

# The Structure of Ditin(II) Oxide Sulfate

BY GEORG LUNDGREN, GUNNAR WERNFORS AND TOSHIO YAMAGUCHI

Department of Inorganic Chemistry, Chalmers University of Technology and the University of Göteborg, S-412 96 Göteborg, Sweden

### Abstract

Sn$_2$OSO$_4$ crystallizes in the tetragonal space group $P42_1c$ with $a = 10.930$ (2), $c = 8.931$ (2) Å, $V = 1067$ (2) Å$^3$ and $Z = 8$. The structure has been refined to a final $R = 0.049$ for 1796 significant diffractometer reflections. A three-dimensional structure is built up by the linkage of Sn$_8$O$_4^{8+}$ groups through sulfate ions. The two independent Sn atoms have an O coordination intermediate between three- and fourfold, both having three shorter Sn—O bonds in the range 2.137 (6)–2.353 (6) Å, and one longer of 2.523 (8) and 2.562 (8) Å, respectively. The sulfate group has S—O distances in the range 1.448 (8)–1.488 (7) Å.

## Introduction

Basic salts of $Sn^{II}$ were investigated by Tobias (1958) by potentiometric measurements. He found that the complex $Sn_3(OH)_4^{2+}$ dominates with small amounts of $SnOH^+$ and $Sn_2(OH)_2^{2+}$ present at rather high tin concentrations. The formation of the predominant $Sn_3(OH)_4^{2+}$ complex was later confirmed by other workers (Liang & Tu, 1964; Gobom, 1976). A probable model of the structure of the $Sn_3(OH)_4^{2+}$ complex has been proposed from X-ray scattering measurements of concentrated hydrolyzed tin(II) per-chlorate solutions (Johansson & Ohtaki, 1973). Only a few crystal structure determinations of basic $Sn^{II}$ salts have been carried out so far: $Sn_2O(OH)_2SO_4$ (Davies, Donaldson, Laughlin, Howie & Beddoes, 1975; Grim-vall, 1975), $Sn_2(OH)PO_4$ (Jordan, Schroeder, Dickens & Brown, 1976), $Sn_3O(OH)PO_4$ (Jordan, Dickens, Schroeder & Brown, 1980).

In a previous investigation of the structure of $Sn_2OSO_4$, the positions of the Sn atoms were deter-mined (Wernfors, 1961). From this study it was clear that the structure is not isomorphous with the cor-responding lead salt, $Pb_2OSO_4$. In the present in-vestigation, the complete $Sn_2OSO_4$ structure has been determined from diffractometer data.

## Experimental

Crystals of $Sn_2OSO_4$ were prepared by hydrothermal synthesis, as described in a previous paper (Wernfors, 1961). The crystals are very sensitive to oxidation in air, and their surfaces turned grey within 10 min in air.

An irregular crystal was sealed in a glass capillary and mounted on a four-circle Syntex $P2_1$ diffractom-eter. Intensity data were collected at 294 K for $h,k,l \geq 0$ with a variable scan speed. Two standard reflections monitored after every fiftieth reflection showed that the crystal was stable in the capillary during data collec-tion. Diffraction data were recorded in 96-step profiles for each reflection and the net intensities were evaluated by the Lehmann & Larsen (1974) profile-analysis method (program $LELA$; Lindqvist & Ljungström, 1979). Following the data collection, a series of $\psi$ scans around the diffraction vector of ten reflections were recorded in the $2\theta$ range 8–58°, and used in an empirical absorption correction (program $TAPER$; Syntex, 1973).

Reflections with $I \geq 3\sigma(I)$ were regarded as significant and corrected for Lorentz and polarization effects. Experimental details are summarized in Table 1.

## Structure determination

Initially, the previously reported (Wernfors, 1961) positional parameters of Sn were refined. Successive difference Fourier summations revealed all the other atoms in the structure. With anisotropic thermal parameters for all atoms, a block-diagonal least-squares refinement (program $BLOCK$; Lindgren, 1977) of the model gave a final $R = 0.049$. An iso-tropic-extinction correction (Zachariasen, 1967) was applied and the $g$ value was fixed in the refinement. The weighting scheme $w = 1/(20.0 + |F_o| + 0.011|F_o|^2 + 0.0002|F_o|^3)$ gave an acceptable weight analysis. A final difference synthesis showed no anomalies. Scatter-ing factors for neutral Sn, S and O were taken from *International Tables for X-ray Crystallography* (1974). Final positional and equivalent isotropic thermal parameters are given in Table 2.* Calculations were performed on an Hp 2100 computer with the use of a modified Syntex $XTL$ program package (Syntex, 1973; Sjölin, 1979).

---

Table 1. *Crystal data, and details of the collection and reduction of intensities and of the least-squares refinements*

| | | | |
|---|---|---|---|
| Formula | $Sn_2OSO_4$ | Scan interval, $\Delta\theta$ (°) | $[(Mo\ K\alpha_2) + 1.00]$–$[(Mo\ K\alpha_1) - 1.00]$ |
| FW | 349.4 | Reflections recorded | 2550 |
| $D_x$ (Mg m$^{-3}$) | 4.35 | Significant reflections | 1796 $[I/\sigma(I) > 3.0]$ |
| $F(000)$ | 1248 | Parameters refined | 74 |
| Crystal habit | Colourless and irregular | $R = \sum \|F_o\| - \|F_c\|\|/\sum \|F_o\|$ | 0.049 ($R = 0.065$ including unobserved |
| Crystal size (mm) | $0.10 \times 0.12 \times 0.15$ | | reflections) |
| Radiation | Mo $K\alpha$ ($\lambda = 0.71069$ Å) | $\mu$(Mo $K\alpha$) (mm$^{-1}$) | 9.70 |
| Monochromator | Graphite crystal | Range of transmission factor | 0.752–0.997* |
| Scan mode | $\theta$–$2\theta$ | $g$ (isotropic extinction parameter) | 0.005 |
| Maximum $2\theta$ (°) | 70 | | |
| Scan speed (° min$^{-1}$) | Variable, 3.0–20.0 | | |

* Values calculated from measured intensities.

Table 2. *Positional parameters and equivalent iso-tropic thermal parameters, with e.s.d.'s in parentheses*

|        | $x$ | $y$ | $z$ | $B_{eq}$ (Å$^2$)* |
|--------|-----|-----|-----|-------|
| Sn(1) | 0·99364 (5) | 0·16119 (5) | 0·13650 (3) | 1·391 (7) |
| Sn(2) | 0·29045 (5) | 0·01554 (5) | 0·24191 (7) | 1·523 (7) |
| S     | 0·2928 (2)  | 0·2946 (2)  | 0·0058 (3)  | 1·29 (3) |
| O(1)  | 0·1259 (5)  | 0·0168 (5)  | 0·1128 (6)  | 1·10 (8) |
| O(2)  | 0·3469 (7)  | 0·1814 (7)  | 0·0580 (8)  | 2·10 (11) |
| O(3)  | 0·1588 (7)  | 0·2880 (7)  | 0·0048 (10) | 2·27 (12) |
| O(4)  | 0·3330 (7)  | 0·3975 (7)  | 0·1001 (9)  | 2·09 (11) |
| O(5)  | 0·3335 (7)  | 0·3147 (7)  | −0·1512 (7) | 2·01 (11) |

$$* \; B_{eq} = \tfrac{4}{3} \textstyle\sum_i \sum_j \beta_{ij} \, \mathbf{a}_i \cdot \mathbf{a}_j.$$

## Description of the structure and discussion

### Structural build-up

The structure contains one $SO_4^{2-}$, one $O^{2-}$ and two unique $Sn^{2+}$ ions. Fig. 1 shows a stereoscopic view of the unit cell of the structure.

The characteristic feature of the structure is the presence of $Sn_8O_4$ groups (*cf.* Fig. 2). Within such a group, four Sn(1) atoms form an almost regular tetrahedron, while the remaining four Sn(2) atoms are situated on the faces of the Sn(1) tetrahedra in such a way that one Sn(2) and three Sn(1) form another almost regular tetrahedron (Fig. 2). The four O atoms are situated approximately at the centers of these outer Sn tetrahedra. In the structure of $Sn_2OSO_4$, each $Sn_8O_4$ group is connected to four sulfate groups. In each sulfate group two O atoms, O(2) and O(3), are in contact with one $Sn_8O_4$ group, whereas the remaining two, O(4) and O(5), are joined to two other $Sn_8O_4$ groups, resulting in a three-dimensional network (Fig. 1).

### Sn coordination

The environments of the two independent Sn$^{II}$ atoms are shown in Fig. 3 and details are given in Table 3.

The O coordinations are rather similar around the two independent Sn atoms. Each Sn atom forms three short bonds to O atoms (2·137–2·353 Å), one intermediate bond (2·523–2·562 Å) and two or three longer interactions (2·826–3·286 Å). The three O atoms strongly bonded to Sn(1) are oxide ions, O(1), whereas the Sn(2) atom is bonded to one oxide ion, O(1), and to two $SO_4^{2-}$ O atoms, O(4) and O(5).

The O coordinations around both Sn atoms are thus basically threefold, having elements of fourfold
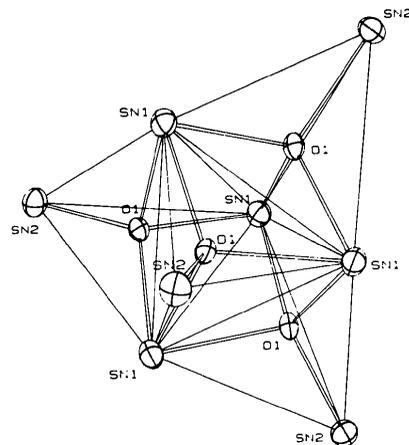
Fig. 2. The $Sn_8O_4$ unit.
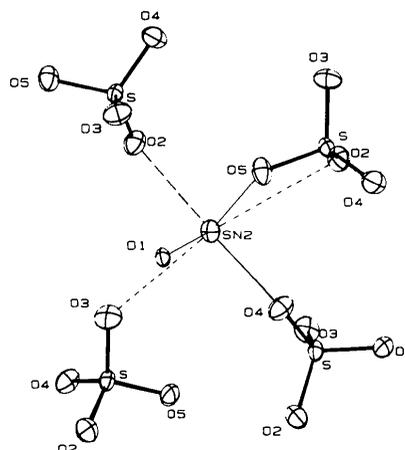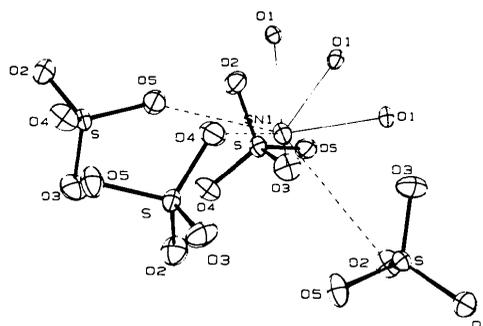
Fig. 3. The Sn(1) and Sn(2) coordination environments.

Fig. 1. Stereoscopic view of the structure of $Sn_2OSO_4$.

Table 3. *Interatomic distances (Å) and angles (°) with e.s.d.'s in parentheses*

(a) Sn(1) coordination

| | | | |
|---|---|---|---|
| Sn(1)–O(1$^i$) | 2·150 (6) | O(1$^i$)–Sn(1)–O(1$^{ii}$) | 79·2 (2) |
| Sn(1)–O(1$^{ii}$) | 2·262 (5) | O(1$^i$)–Sn(1)–O(1$^{iii}$) | 76·0 (2) |
| Sn(1)–O(1$^{iii}$) | 2·353 (6) | O(1$^i$)–Sn(1)–O(3$^i$) | 83·0 (2) |
| Sn(1)–O(3$^i$) | 2·562 (8) | O(1$^{ii}$)–Sn(1)–O(1$^{iii}$) | 75·1 (2) |
| Sn(1)–O(5$^{iv}$) | 2·826 (7) | O(1$^{ii}$)–Sn(1)–O(3$^i$) | 71·1 (2) |
| Sn(1)–O(4$^v$) | 3·005 (8) | O(1$^{iii}$)–Sn(1)–O(3$^i$) | 142·9 (2) |
| Sn(1)–O(2$^{ii}$) | 3·286 (8) | | |
| O(1$^i$)–O(1$^{ii}$) | 2·813 (9) | O(1$^{ii}$)–O(1$^{iii}$) | 2·813 (9) |
| O(1$^i$)–O(1$^{iii}$) | 2·777 (12) | O(1$^{ii}$)–O(3$^i$) | 2·815 (9) |
| O(1$^i$)–O(3$^i$) | 3·137 (9) | | |

(b) Sn(2) coordination

| | | | |
|---|---|---|---|
| Sn(2)–O(1) | 2·137 (6) | O(1)–Sn(2)–O(2) | 81·4 (2) |
| Sn(2)–O(5$^{vi}$) | 2·226 (8) | O(1)–Sn(2)–O(4$^{vii}$) | 81·0 (2) |
| Sn(2)–O(4$^{vii}$) | 2·340 (8) | O(1)–Sn(2)–O(5$^{vi}$) | 78·0 (2) |
| Sn(2)–O(2) | 2·523 (8) | O(2)–Sn(2)–O(4$^{vii}$) | 158·4 (3) |
| Sn(2)–O(3$^{viii}$) | 2·913 (9) | O(4$^{vii}$)–Sn(2)–O(5$^{vi}$) | 81·5 (3) |
| Sn(2)–O(2$^{ix}$) | 3·213 (8) | O(2)–Sn(2)–O(5$^{vi}$) | 82·7 (3) |
| O(1)–O(5$^{vi}$) | 2·746 (9) | O(5$^{vi}$)–O(4$^{vii}$) | 2·982 (11) |
| O(1)–O(4$^{vii}$) | 2·912 (10) | O(5$^{vi}$)–O(2) | 3·145 (10) |
| O(1)–O(2) | 3·051 (10) | | |

(c) The SO$_4^{2-}$ group

| | | | |
|---|---|---|---|
| S–O(2) | 1·448 (8) | O(2)–S–O(3) | 111·6 (5) |
| S–O(3) | 1·466 (8) | O(2)–S–O(4) | 110·3 (5) |
| S–O(4) | 1·472 (8) | O(2)–S–O(5) | 107·9 (4) |
| S–O(5) | 1·488 (7) | O(3)–S–O(4) | 109·9 (5) |
| | | O(3)–S–O(5) | 107·4 (5) |
| | | O(4)–S–O(5) | 109·7 (5) |
| O(2)–O(3) | 2·410 (11) | O(3)–O(4) | 2·405 (11) |
| O(2)–O(4) | 2·396 (11) | O(3)–O(5) | 2·381 (11) |
| O(2)–O(5) | 2·374 (10) | O(4)–O(5) | 2·420 (10) |

(d) The Sn$_8$O$_4$ group

| | | | |
|---|---|---|---|
| O(1)–Sn(1$^x$) | 2·150 (6) | Sn(2)–O(1)–Sn(1$^x$) | 121·2 (3) |
| O(1)–Sn(1$^{iii}$) | 2·353 (6) | Sn(2)–O(1)–Sn(1$^{xi}$) | 112·8 (3) |
| O(1)–Sn(1$^{xi}$) | 2·262 (5) | Sn(2)–O(1)–Sn(1$^{iii}$) | 114·4 (2) |
| O(1)–Sn(2) | 2·137 (6) | Sn(1$^x$)–O(1)–Sn(1$^{xi}$) | 104·4 (2) |
| Sn(1$^x$)–Sn(1$^{iii}$) | 3·526 (1) | Sn(1$^x$)–O(1)–Sn(1$^{iii}$) | 103·0 (2) |
| Sn(1$^x$)–Sn(1$^{xi}$) | 3·487 (1) | Sn(1$^{xi}$)–O(1)–Sn(1$^{iii}$) | 98·1 (2) |
| Sn(1$^x$)–Sn(2) | 3·734 (1) | Sn(1$^{xi}$)–Sn(2) | 3·664 (1) |
| Sn(1$^{iii}$)–Sn(1$^{xi}$) | 3·487 (1) | | |
| Sn(1$^{iii}$)–Sn(2) | 3·776 (1) | | |

Symmetry code

| | | | |
|---|---|---|---|
| (i) | $1 + x, y, z$ | (ii) | $1 - y, x, -z$ |
| (iii) | $1 - x, -y, z$ | (iv) | $\frac{3}{2} - y, \frac{1}{2} - y, \frac{1}{2} + z$ |
| (v) | $\frac{1}{2} + x, \frac{1}{2} - y, \frac{1}{2} - z$ | (vi) | $\frac{1}{2} - y, \frac{1}{2} - x, \frac{1}{2} + z$ |
| (vii) | $\frac{1}{2} - x, -\frac{1}{2} + y, \frac{1}{2} - z$ | (viii) | $y, -x, -z$ |
| (ix) | $\frac{1}{2} - y, \frac{1}{2} - x, \frac{1}{2} + z$ | (x) | $-1 + x, y, z$ |
| (xi) | $y, 1 - x, -z$ | | |

trigonal-bipyramidal geometry (*cf.* Table 3). In the typical fourfold trigonal-bipyramidal configuration the trigonal base plane contains two short bonds (Sn–O $\simeq$ 2·20 Å and O–Sn–O $\simeq$ 95°) and the Sn$^{II}$ lone pair, while there are two longer bonds in the axial direction (Sn–O $\simeq$ 2·45 Å and O–Sn–O $\simeq$ 155°) (Yamaguchi & Lindqvist, 1982). The stereochemical activity of the Sn$^{II}$ lone pair of electrons is evident, since the four strongest coordinated O atoms are situated within one hemisphere in both cases. This is consistent with the general view of tin(II)–oxygen compounds (Zubieta & Zuckermann, 1978).

## The sulfate group

The details of the sulfate group are given in Table 3. The S–O(4) and S–O(5) bond distances are significantly longer than the other two S–O bonds. This is probably because O(4) and O(5) are strongly bonded to the Sn atoms, while O(2) and O(3) have weaker interactions with Sn (*cf.* Table 3). The mean S–O bond distance of 1·469 (8) Å is consistent with most values reported in the literature. The mean O–S–O bond angle is 109·5° and the individual O–S–O angles deviate little from tetrahedral geometry.

## The oxide ion

The environment of the oxide ion, O(1), is shown in Fig. 2 and the details are given in Table 3. The oxide ion is strongly bonded to three Sn(1) atoms and one Sn(2), forming a distorted tetrahedron. The mean Sn–O–Sn angle is 109·0°.

## Comparison with structures of some basic Pb$^{II}$ salts

Sahl (1970) determined the structure of Pb$_2$OSO$_4$ in space group $C2/m$. In this structure, the oxide ion is surrounded by four Pb atoms, similar to the Sn$_4$O unit in the present compound. The O coordinations of the two unique Pb atoms are essentially threefold (Pb–O distances of 2·30–2·55 Å), which is also similar to the Sn–O coordination in the Sn$_2$OSO$_4$ structure. There are two intermediate Pb–O bonds of 2·78–2·82 Å completing a distorted fivefold coordination in Pb$_2$OSO$_4$.

The greatest difference between the two structures involves the connections between the PbO$_4$ and SnO$_4$ units, respectively. Pb$_2$OSO$_4$ does not contain any Pb$_8$O$_4$ groups, but the Pb tetrahedra share edges to form infinite chains. These chains are connected by sulfate groups to form planes with only weak bonds between the planes. The differences between the two structures are probably due to the higher stereochemical activity of the Sn$^{II}$ lone-pair electrons.

The central Sn$_4$ unit in the Sn$_8$O$_4$ cluster is also related to that of Pb$_4$(OH)$_4^{4+}$ (Hong & Olin, 1973), in which the Pb atoms form a single tetrahedron, and to that of Pb$_6$O(OH)$_6^{4+}$ (Spiro, Templeton & Zalkin, 1968), in which four Pb atoms form a tetrahedron, two faces of which are connected by two extra Pb atoms.

## References

DAVIES, C. G., DONALDSON, J. D., LAUGHLIN, D. R., HOWIE, R. A. & BEDDOES, R. (1975). *J. Chem. Soc. Dalton Trans.* pp. 2241–2244.

GOBOM, S. (1976). Acta Chem. Scand. Ser. A, 30, 745–750.

GRIMVALL, S. (1975). Acta Chem. Scand. Ser. A, 29, 590–598.

HONG, S.-H. & OLIN, Å. (1973). Acta Chem. Scand. 27, 2309–2320.

International Tables for X-ray Crystallography (1974). Vol. IV. Birmingham: Kynoch Press.

JOHANSSON, G. & OHTAKI, H. (1973). Acta Chem. Scand. 27, 643–660.

JORDAN, T. H., DICKENS, B., SCHROEDER, L. W. & BROWN, W. E. (1980). Inorg. Chem. 19, 2551–2556.

JORDAN, T. H., SCHROEDER, L. W., DICKENS, B. & BROWN, W. E. (1976). Inorg. Chem. 15, 1810–1814.

LEHMANN, M. S. & LARSEN, F. K. (1974). Acta Cryst. A30, 580–584.

LIANG, C.-C. & TU, Y.-M. (1964). Russ. J. Inorg. Chem. 9, 727.

LINDGREN, O. (1977). Thesis, Univ. of Göteborg.

LINDQVIST, O. & LJUNGSTRÖM, E. (1979). J. Appl. Cryst. 12, 134.

SAHL, K. (1970). Z. Kristallogr. 132, 99–117.

SJÖLIN, L. (1979). Thesis, Univ. of Göteborg.

SPIRO, T. G., TEMPLETON, D. H. & ZALKIN, A. (1968). Inorg. Chem. 8, 856–861.

Syntex (1973). The XTL structure determination package. Syntex, 10040 Bubb Road, Cupertino, California 95015.

TOBIAS, R. S. (1958). Acta Chem. Scand. 12, 198–223.

WERNFORS, G. (1961). Acta Chem. Scand. 15, 1007–1016.

YAMAGUCHI, T. & LINDQVIST, O. (1982). Acta Cryst. B38, 1441–1445.

ZACHARIASEN, W. H. (1967). Acta Cryst. 23, 558–564.

ZUBIETA, J. A. & ZUCKERMANN, J. J. (1978). Prog. Inorg. Chem. 24, 251–475.

---

# Relationship between Crystal Structure and Ionic Conductivity in CuTeBr

BY R. BACHMANN, K. D. KREUER, A. RABENAU AND H. SCHULZ

Max-Planck-Institut für Festkörperforschung, Heisenbergstrasse 1, D-7000 Stuttgart 80,
Federal Republic of Germany

## Abstract

The high-temperature structure of CuTeBr, which exhibits fast ionic conduction, was investigated by single-crystal X-ray diffraction at 373 and 473 K. [Space group $I4_1/amd$; $T = 373$ K: $a = 16\cdot334$ (3), $c = 4\cdot785$ (2) Å, $R_w(F) = 1\cdot2\%$, 303 observed reflections; $T = 473$ K: $a = 16\cdot396$ (5), $c = 4\cdot776$ (3) Å, $R_w(F) = 1\cdot2\%$, 283 observed reflections.] The investigation revealed that the ionic conduction has to be highly anisotropic. A conduction path was found parallel to the $c$ axis. From the refined anharmonic temperature factors a potential barrier of $0\cdot1$ eV (1 eV $\equiv 1\cdot6 \times 10^{-19}$ J) was calculated for the motion of copper ions along this path. Conductivity measurements of single crystals confirmed the high anisotropy. At 473 K the conductivity parallel to the $c$ axis is $0\cdot15$ $\Omega^{-1}$ cm$^{-1}$ with an activation energy of $0\cdot25$ eV. This is more than ten times the conductivity perpendicular to the $c$ axis, which has an activation energy of $0\cdot36$ eV.

## Introduction

The three isotypic compounds CuTe$X$ ($X$ = Cl, Br, I) all exhibit a high copper(I) ionic conductivity (von Alpen, Fenner, Marcoll & Rabenau, 1977) and all are fast ionic conductors at temperatures above 400 K. Among them, CuTeBr has the highest ionic conductivity and lowest activation energy. The low activation energy enables us to study the conduction mechanism with the aid of elastic X-ray diffraction at elevated temperatures. Therefore, the high-temperature structure of CuTeBr was reinvestigated using intensities collected at 373 and 473 K.

## Experimental

CuTeBr was prepared by annealing stoichiometric amounts of Te (99·999% pure) and twice-distilled CuBr at a temperature of 623 K for two weeks. Single crystals were grown by the Bridgeman technique. The evacuated ampoule was heated to 753 K and lowered into a Bridgeman furnace at a rate of 10 mm d$^{-1}$. The crystals obtained were pin shaped, up to 2 cm long and a few mm in diameter. Large single crystals with a diameter of more than 1 cm were grown by a modified Bridgeman technique (Lamprecht & Geiger, 1982).

The crystal used for the X-ray measurement was $0\cdot06 \times 0\cdot06 \times 0\cdot12$ mm. The data collection was carried out with a Philips PW 1100 four-circle